Dalton Transactions

PAPER

View Article Online
View Journal | View Issue

Cite this: *Dalton Trans.*, 2016, **45**, 17874

Systematic XAS study on the reduction and uptake of Tc by magnetite and mackinawite†

Ezgi Yalçıntaş,*[a] Andreas C. Scheinost,*[b,c] Xavier Gaona[a] and Marcus Altmaier[a]

Received 20th July 2016,
Accepted 18th October 2016

DOI: 10.1039/c6dt02872a

www.rsc.org/dalton

The mechanisms for the reduction and uptake of Tc by magnetite (Fe_3O_4) and mackinawite (FeS) are investigated using X-ray absorption spectroscopy (XANES and EXAFS), in combination with thermodynamic calculations of the Tc/Fe systems and accurate characterization of the solution properties (pH_m, pe, [Tc]). Batch sorption experiments were performed under strictly anoxic conditions using freshly prepared magnetite and mackinawite in 0.1 M NaCl solutions with varying initial Tc(VII) concentrations (2×10^{-5} and 2×10^{-4} M) and Tc loadings (400–900 ppm). XANES confirms the complete reduction of Tc(VII) to Tc(IV) in all investigated systems, as predicted from experimental (pH_m + pe) measurements and thermodynamic calculations. Two Tc endmember species are identified by EXAFS in the magnetite system, Tc substituting for Fe in the magnetite structure and Tc–Tc dimers sorbed to the magnetite {111} faces through a triple bond. The sorption endmember is favoured at higher [Tc], whereas incorporation prevails at low [Tc] and less alkaline pH conditions. The key role of pH in the uptake mechanism is interpreted in terms of magnetite solubility, with higher [Fe] and greater recrystallization rates occurring at lower pH values. A TcS_x-like phase is predominant in all investigated mackinawite systems, although the contribution of up to 20% of $TcO_2{\cdot}xH_2O$(s) (likely as surface precipitate) is observed for the highest investigated loadings (900 ppm). These results provide key inputs for an accurate mechanistic interpretation of the Tc uptake by magnetite and mackinawite, so far controversially discussed in the literature, and represent a highly relevant contribution to the investigation of Tc retention processes in the context of nuclear waste disposal.

Introduction

Technetium-99 is a β-emitting fission product highly relevant in the safety assessment of repositories for radioactive waste disposal due to its significant inventory in spent nuclear fuel, long half-life ($t_{1/2} \sim 2.1 \times 10^5$ a) and redox-sensitive chemical behaviour. Although several oxidation states of Tc are reported in the literature (from 0 to +VII),[1–5] Tc(VII) and Tc(IV) are the prevailing redox states in the absence of any complexing ligand other than water under non reducing and reducing conditions, respectively. Tc(VII) is the most stable oxidation state of Tc in suboxic/oxidising environments, it is found as the highly mobile TcO_4^- anion over the entire pH range and shows very high solubility and weak sorption properties.[5] Under reducing conditions, Tc(IV) forms sparingly soluble hydrous oxides $TcO_2{\cdot}xH_2O$(s) and is strongly sorbed onto mineral surfaces.[6–13] Because of the large differences in the aquatic chemistry of Tc(VII) and Tc(IV), an accurate knowledge of Tc redox chemistry is necessary for an appropriate assessment of Tc retention/mobilization processes under repository-relevant conditions.

As for other redox-sensitive radionuclides, Fe(II) solid phases play a relevant role in the (geo)chemistry of Tc, often involving a combination of reduction and uptake processes. Indeed, the release of Fe(II) through the anoxic corrosion of metallic iron/steel canisters and the corresponding formation of Fe(II) minerals play a very important role in defining the redox boundary conditions of deep underground repositories for the disposal of radioactive waste, whilst having also a great impact on the uptake of radionuclides. Magnetite (Fe_3O_4) and mackinawite (FeS) are corrosion products of Fe expected to form under repository-relevant conditions. Magnetite is the most relevant Fe(II)–Fe(III) mixed oxide and shows a very large stability field ranging from near-neutral to hyperalkaline pH conditions. In spite of this, relevant uncertainties still exist for the thermodynamic data available for this compound, mainly resulting from kinetically controlled solubility behaviour at T = 25 °C and with regard to crystallinity and particle size. Mackinawite is an Fe(II)–sulphide phase found in certain types[14,15] of clay formations (*e.g.* Callovo Oxfordian) and

[a]*Institute for Nuclear Waste Disposal, Karlsruhe Institute of Technology, Germany. E-mail: ezgi.yalcintas@kit.edu*
[b]*Institute of Resource Ecology, Helmholtz-Zentrum Dresden – Rossendorf, Germany*
[c]*The Rossendorf Beamline at ESRF, Grenoble, France. E-mail: scheinost@esrf.fr*
†Electronic supplementary information (ESI) available. See DOI: 10.1039/c6dt02872a

forming in sulphide-rich reducing groundwaters. It occurs naturally as $Fe_{1+x}S$ due to the non-stoichiometric contribution of Ni or Cu (among other) impurities, although it is readily produced as stoichiometric FeS under laboratory conditions.

The role of Fe-containing minerals in the reduction of Tc(VII) has been intensively investigated over the last decades. Cui *et al.* (1996a, b) studied the reduction of Tc(VII) by Fe(II) and the uptake of Tc by magnetite in the presence of synthetic ground water.[16,17] The authors assessed the effect of ionic strength and pH (7.8–9.5), investigated the rate of the sorption reaction, and concluded that the uptake was controlled by a ligand exchange mechanism with a very strong pH-dependency. A number of studies were also dedicated to the interaction of Tc(VII) with Fe-bearing sediments (Wildung *et al.* (2004),[9] Burke *et al.* (2005),[11] Burke *et al.* (2006),[10] McBeth *et al.* (2007),[13] Morris *et al.* (2008),[18] Burke *et al.* (2010),[12] Peretyazhko *et al.* (2012)[7]). All these studies reported the precipitation of $TcO_2{\cdot}xH_2O$(s) as main mechanism for the immobilization of Tc. Geraedts *et al.* (2002, 2008)[19,20] and Maes *et al.* (2004)[21] studied the system magnetite-Tc in the presence of natural and synthetic Gorleben groundwater. The authors observed the formation of $TcO_2{\cdot}xH_2O$(s) in this system, and suggested that Tc(IV) polymers or colloids were responsible for the observed increase in solubility from $\sim10^{-8.5}$ M to $\sim10^{-6}$ M. Kobayashi and co-workers[22] investigated the reduction/sorption of Tc(VII) in the presence of Fe(II) (magnetite, mackinawite and siderite) and Fe(III) (goethite and hematite) minerals. The reduction and consequent decrease in [Tc] were only observed in the presence of the Fe(II) minerals. The authors reported the complete incorporation of Tc(IV) into the magnetite structure, whilst suggesting the formation of a TcS_x-like phase in the mackinawite samples. Marshall *et al.* (2014)[23] investigated the sorption and incorporation of Tc on magnetite in synthetic cement leachates under alkaline pH conditions. The authors reported the predominance of TcO_2 solid phases in the sorption samples. The relevant contribution of Tc–Fe bonds confirmed by EXAFS hinted towards the sorption of Tc-chains on the surface of magnetite, possibly in combination with a partial incorporation in the structure of magnetite. On the contrary, the very large Tc–Fe coordination numbers observed in the coprecipitation samples suggested that incorporation of Tc(IV) into the magnetite structure was the main retention mechanism in this case. In our recent study on the redox behaviour of Tc in the presence of different reducing systems, complete and fast reduction of Tc(VII) to Tc(IV) was observed in the presence of magnetite, mackinawite and siderite in highly saline systems (5.0 M NaCl and 4.5 M $MgCl_2$). XANES analysis of these samples suggested *O*-coordination in the first shell of all investigated samples.[24] Recently, Smith *et al.* (2016) performed quantum chemical calculations to assess the charge-compensation mechanism governing Tc(IV) incorporation in the structure of magnetite.[25] The authors reported that incorporation of Tc(IV) by removing two octahedral Fe(II) ions is energetically favoured. Wharton *et al.* (2000)[26] studied the coprecipitation of Tc(VII) and Tc(IV) with mackinawite and characterized the resulting solid phases by X-ray absorption spectroscopy. Tc was immobilized as a $Tc^{IV}S_2$-like phase regardless of the initial oxidation state of Tc. Similar observations were reported by Livens *et al.* (2004),[27] who investigated the interaction between Tc and mackinawite using both +VII and +IV as initial redox state of Tc. Liu *et al.* (2008)[28] performed comprehensive immobilization experiments with Tc in the presence of mackinawite. The authors assessed the effect of ionic strength (≤1.0 M NaCl) and pH (6.1–9.0) on the uptake of Tc, and observed a strong pH-dependency and the increase of the uptake rate with increasing ionic strength. In contrast to Livens and co-workers, TcO_2-like instead of TcS_2-like phases were reported to form on the surface of mackinawite. Recently, Lee *et al.* (2014) investigated the reduction of Tc by sulphide bearing sediments. These authors also reported the very slow formation of a TcS_x-phase under the investigated conditions.

In spite of the number of publications dedicated to the study of Tc uptake by magnetite and mackinawite, significant contradictions arise in the retention mechanisms proposed in the literature. The lack of extensive studies with systematic variation of key parameters such as [Tc], solid-to-liquid ratio (S : L) or loading importantly hinders a correct and complete evaluation of these mechanism. These uncertainties are tackled in the present work with a combination of classical wet-chemistry methods, thermodynamic calculations (involving Tc/Fe) and advanced spectroscopic techniques.

Experimental

Chemicals

All the experiments and sample preparation were performed in an Ar-glovebox at $T = 22 \pm 2$ °C. All solutions were prepared with purified water (Milli-Q academic, Millipore) and purged with Ar before use to remove traces of oxygen. A purified and radiochemically well-characterized ^{99}Tc stock solution (1.3 M $NaTcO_4$) was used for the experiments after dilution to 20 mM with Milli-Q water. NaCl (p.a.) and Na_2S were obtained from Merck; $FeCl_3{\cdot}6H_2O$, $Fe(NH_4)_2(SO_4)_2{\cdot}6H_2O$ and NH_4OH were obtained from Sigma-Aldrich, and $FeCl_2$ from Alfa Aesar.

Fe minerals

Magnetite and mackinawite were synthesized following the well-established methods reported in ref. 29–32 (experimental description summarized in Table S1 in the ESI†). Both solid phases were equilibrated for 4 weeks in the original synthesis solution, washed three times with the corresponding background electrolyte (0.1 M NaCl) and equilibrated in this solution for 3 weeks. The resulting solids were characterized by powder X-ray diffraction (D8 ADVANCE, Bruker) before and after washing with the respective background electrolyte solutions to confirm that solids remained the same during the equilibration. XRD measurements were performed at $10° \leq 2\theta \leq 78°$ with incremental steps of 0.015° and a measurement time of 1.7 seconds per step. The XRD patterns of the Fe phases synthesized in this work are shown in Fig. S1 in the

ESI.† The comparison of these patterns with peak positions and relative intensities reported for magnetite and mackinawite reference materials (JCPDS PDF files 19-0629[33] and 15-0037[34]) unequivocally confirm the predominance of these phases in the synthesized materials. The XRD line widths as well as the SEM micrographs (Fig. S2†) confirm the previously observed nanocrystalline nature of the minerals synthesized this way. Magnetite is characterized by aggregates of small particles, whereas mackinawite shows a platelet-based structure. In both cases, particle sizes agrees well with data previously reported for Fe minerals synthesized by the same method.[29,31,35] Note that the crystallinity of the magnetite synthesized in this work is significantly lower (*e.g.* smaller particle size) than such obtained using the standard method described by Schwertmann and Cornell[36] at T = 80 °C.

pH and E_h measurements

Combination pH electrodes (type ROSS, Orion) calibrated against standard pH buffers (pH = 1–12, Merck) were used to measure the hydrogen ion concentration ($pH_m = -\log m_{H^+}$). The pH_m values were calculated by adding empirical correction factors A_m, which are significant in saline systems at $I \geq 0.1$ m, to the operational "measured" pH_{exp} values ($pH_m = pH_{exp} + A_m$).[37]

Redox potentials were measured with Pt combination electrodes with Ag/AgCl reference system (Metrohm) and converted to E_h *versus* the standard hydrogen electrode by correction for the potential of the Ag/AgCl reference electrode (+208 mV for 3.0 M KCl at T = 22 °C). Stable E_h readings were recorded within 30 minutes by continuous agitation. The apparent electron activity ($pe = -\log a_{e^-}$) was calculated from $E_h = -(RT/F)\ln a_{e^-}$, according to the relation $pe = 16.9\ E_h$ (V). The performance of the redox electrode was tested with a standard redox buffer solution (Schott, +220 mV *vs.* Ag/AgCl), which provided readings within ±10 mV of the certified value.

Sample preparation

The uptake of Tc by magnetite and mackinawite suspensions was investigated as a function of the initial TcO_4^- concentration (2×10^{-4} M and 2×10^{-5} M) and Tc loading on Fe minerals (400 ppm, 600 ppm and 900 ppm, obtained by decreasing solid-to-liquid ratios). Experimental conditions used in the sample preparation are summarized in Table 1. After the addition of Tc, samples were equilibrated under Ar atmosphere for 6 weeks and pH_m, E_h and [Tc] (after 10 kD ultrafiltration) were measured. Magnetite and mackinawite samples with the highest amount of Tc ($[TcO_4^-]_0 = 2 \times 10^{-4}$ M and 900 ppm loading) (~0.5 mg each) were analysed by SEM to assess the morphology of the Fe phases responsible for the retention of Tc.

$TcO_2{\cdot}xH_2O$ used as reference material in the fitting procedure was prepared by acidifying a pertechnetate solution with concentrated HCl, then adding Zn to generate nascent hydrogen. After the reaction was completed, 20 M NaOH solution as added to obtain a black precipitate, which was aged for one week.[38]

XANES/EXAFS measurements

Sample preparation. After 6 weeks of equilibration time, magnetite and mackinawite reacted with Tc were centrifuged at 4020*g* for 10 min and the supernatant removed. Since both Tc(IV) and Fe(II) minerals are very sensitive to oxygen, all preparation steps were performed with special precautions to avoid/minimize the access of air to the samples. The wet paste material resulting from phase separation was placed in a polyethylene (PE) double confined sample holder and heat-sealed inside the Ar-glovebox. Sealed PE sample holders were taken out of the glovebox, immersed in dry ice (−78 °C) to minimize the diffusion of O_2 into the samples, and immediately measured for gamma activity for 30 minutes (mandatory according to European transport regulations and safety protocols). Directly after gamma measurements, the samples were transferred to a liquid N_2-filled Dewar (Voyager 12, Air Liquide – DMC, France). The latter was used to transport the samples

Table 1 Experimental conditions in the Tc reduction/sorption experiments with magnetite (Mag) and mackinawite (Mack) in 0.1 M NaCl systems (before addition of Tc)

Fe minerals	Background electrolyte	$[TcO_4^-]_0$ [b] [M]	Solid/liquid ratio (g L^{-1})	Loading (ppm)	Loading[c] (μmol m^{-2})
Mag-0[a]	0.1 M NaCl	2×10^{-5}	5	400	0.04
Mag-1	0.1 M NaCl	2×10^{-4}	50	400	0.04
Mag-2	0.1 M NaCl	2×10^{-4}	33	600	0.06
Mag-3	0.1 M NaCl	2×10^{-4}	22	900	0.08
Mag-4	0.1 M NaCl	2×10^{-5}	5	400	0.04
Mag-5	0.1 M NaCl	2×10^{-5}	3	600	0.06
Mag-6	0.1 M NaCl	2×10^{-5}	2	900	0.08
Mack-1	0.1 M NaCl	2×10^{-4}	50	400	0.01
Mack-2	0.1 M NaCl	2×10^{-4}	33	600	0.02
Mack-3	0.1 M NaCl	2×10^{-4}	22	900	0.03
Mack-4	0.1 M NaCl	2×10^{-5}	5	400	0.01
Mack-5	0.1 M NaCl	2×10^{-5}	3	600	0.02
Mack-6	0.1 M NaCl	2×10^{-5}	2	900	0.03

[a] Data taken from Kobayashi *et al.* (2013).[22] [b] Initial Tc(VII) concentration. [c] Calculated based on specific surface area of 110 $m^2\ g^{-1}$ for magnetite and 270 $m^2\ g^{-1}$ for mackinawite.[29]

to the synchrotron facility and to store them under conditions where redox transformations or other sample alterations can be excluded. The samples were measured within 20–30 days after preparation for XAFS measurements. Previous studies with redox sensitive elements (Pu, Np, Tc) have shown that storage under liquid nitrogen condition avoids oxidation process (over significantly longer time periods).[22,35,39]

XAFS measurements. Spectra were acquired at the Rossendorf Beamline (BM20 at ESRF) in fluorescence mode at the Tc-K edge (21 044 eV). The energy of the Si(111) double-crystal monochromator was calibrated using a Mo foil (edge energy 20 000 eV). Two Rh-coated mirrors were used to collimate the beam into the monochromator crystal and to reject higher-order harmonics. Fluorescence spectra were collected with a 13-element, high-purity, solid-state Ge detector (Canberra) with digital spectrometer (XIA XMAP). During the measurement, the samples were kept at 15 K with a closed-cycle He cryostat to avoid photon-induced changes of oxidation state and to reduce thermal disorder.[35]

Data evaluation. SIXPACK[40] was used for dead-time correction of the fluorescence data and to average the raw spectra. WinXAS[41] was used for data reduction and analysis following standard procedures. After normalizing the spectra to unity, the energy was converted to photoelectron wave vector units ($Å^{-1}$) by arbitrarily assigning E_0, the origin of the kinetic energy of the photoelectron, to the first inflection point of the absorption edge. The EXAFS $\chi(k)$ functions were then extracted from the post-edge region by using the autospline function of WinXAS. Radial structure functions (RSFs) were obtained by Fourier transforming k^3-weighted $\chi(k)$ functions between 2.0 and 14.5 $Å^{-1}$ using a Bessel function with window parameter 3.

The EXAFS spectra were analysed in a two-step approach. The first step consisted of a statistical analysis of the data based on principal component analysis (PCA) and iterative target-transformation factor analysis (ITFA), using the code developed by A. Rossberg.[42] The procedure is well described in several papers.[42–44] The derivation of the number of spectral components is based on three factors, the minimum of the Malinowski indicator value calculated for all principal components, a visual inspection of the principal components to discriminate the ones which contain the EXAFS signal from those, which arise from fluctuations of the spline background removal and from noise, and finally, and perhaps most important, the reconstruction of the experimental data by a minimum number of components. Varimax rotation and iterative transformation target test using reference spectra as far as available were then performed with ITFA to identify the spectral endmembers and to extract their EXAFS spectra in $k^3\chi(k)$ space for $2.0 \leq k\ [Å^{-1}] \leq 12.5$. In a second step, the EXAFS spectra of the identified principal components were fitted with WinXAS[41] using theoretical backscattering amplitudes and phase shifts calculated with FEFF 8.2.[45] Tc–O, Tc–Fe, Tc–Tc and Tc–S theoretical scattering paths for this shell fit approach were derived by replacing Fe atoms in magnetite and mackinawite structures by Tc. The amplitude reduction factor, S_0^2, was fixed to 0.9 for all fits.

Results and discussion

Quantitative evaluation of the wet chemistry data

Table 2 summarizes the experimentally measured pH_m, E_h and Tc concentrations in the Fe mineral suspensions after 6 weeks of equilibration time. Experimental pH_m and E_h values are also plotted in the Tc Pourbaix diagram shown in Fig. 1. The figure shows that E_h values measured in magnetite samples are slightly below the thermodynamically calculated Tc(VII)/Tc(IV) redox borderline, whereas significantly lower E_h values are found in the mackinawite system. In both cases, Tc concentrations measured in solution decrease to values below the detection limit of LSC (Liquid Scintillation Counting) within 6 weeks, suggesting that TcO_4^- is completely reduced to Tc(IV) and quantitatively removed from the aqueous phase.

Structural interpretation of Tc uptake: EXAFS/XANES

Magnetite. Fig. 2a shows the Tc K-edge XANES spectra of Tc sorbed magnetite samples (labelled Mag-1 to 6) along with the spectra of three references, an amorphous $TcO_2{\cdot}xH_2O$(s) representing the tetravalent oxidation state, Tc(IV) structurally incorporated by magnetite (Mag-0)[22] and the TcO_4^- aquo-complex representing the heptavalent oxidation state of Tc.[47] The XANES spectra of all magnetite samples show edge positions similar to that of Tc(IV) structurally incorporated by magnetite, confirming the reduction of Tc(VII) to Tc(IV). Note that small contributions of Tc(VII) can be excluded, since both the pre-edge peak of Tc(VII) at about 21.05 keV and the white line at 21.10 keV would be easily discernible when exceeding about 5 atom%. The fine structure of all magnetite samples is also very similar, suggesting a Tc coordination similar to Tc(IV) in magnetite, and different from $TcO_2{\cdot}xH_2O$(s). The k^3-weighted EXAFS spectra and the Fourier Transform Magnitudes (FTM) are shown in Fig. 2b and c, respectively. To derive the number of chemically different Tc species in all seven samples based on their short range structure, their EXAFS spectra were inves-

Table 2 Experimentally measured pH_m, E_h and $[Tc]_{final}$ in magnetite (Mag) and mackinawite (Mack) samples after 6 weeks of equilibration time

Fe mineral	pH_m [a]	E_h [b] (mV)	$[Tc]_{final}$ [M]
Mag-0[c]	6.00	−120	$\leq 1 \times 10^{-8}$
Mag-1	9.28	−149	$\leq 4 \times 10^{-10}$ [d]
Mag-2	9.16	−146	$\leq 4 \times 10^{-10}$ [d]
Mag-3	9.08	−139	$\leq 4 \times 10^{-10}$ [d]
Mag-4	9.12	−138	$\leq 4 \times 10^{-10}$ [d]
Mag-5	8.90	−121	$\leq 4 \times 10^{-10}$ [d]
Mag-6	8.68	−109	$\leq 4 \times 10^{-10}$ [d]
Mack-1	9.07	−315	$\leq 4 \times 10^{-10}$ [d]
Mack-2	9.16	−381	$\leq 4 \times 10^{-10}$ [d]
Mack-3	8.99	−309	$\leq 4 \times 10^{-10}$ [d]
Mack-4	9.02	−289	$\leq 4 \times 10^{-10}$ [d]
Mack-5	8.91	−280	$\leq 4 \times 10^{-10}$ [d]
Mack-6	8.83	−271	$\leq 4 \times 10^{-10}$ [d]

[a] ±0.05. [b] ±50 mV. [c] Data taken from Kobayashi *et al.* (2013).[22] [d] Detection limits.

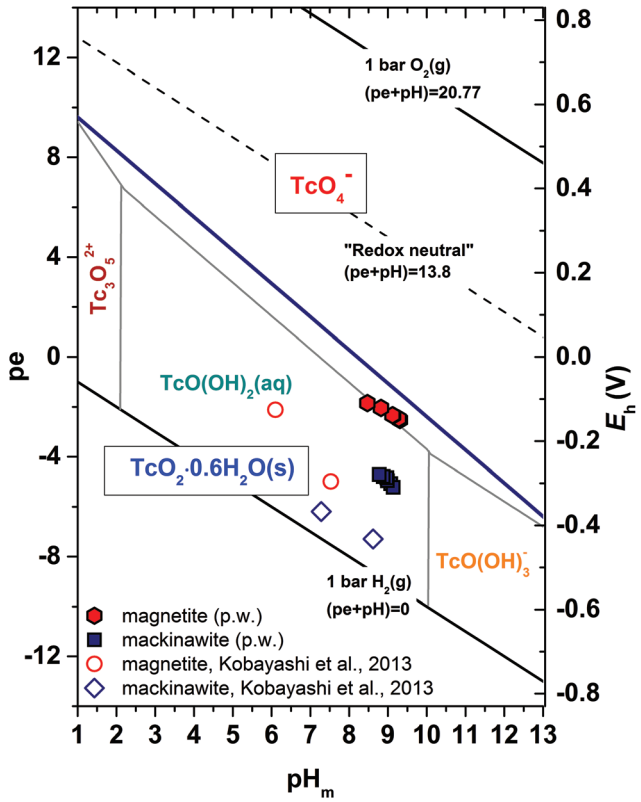

Fig. 1 Experimental pH_m and E_h values of Tc samples in 0.1 M NaCl in the presence of magnetite and mackinawite. Measurements performed after 6 weeks of equilibration time (directly before sampling for EXAFS measurements). Solid blue line represents the 50 : 50 equilibrium line for Tc(VII)/Tc(IV) calculated at I = 0.1 M according to the reaction $TcO_4^- + 4H^+ + 3e^- \Leftrightarrow TcO_2{\cdot}0.6H_2O(s) + 1.4H_2O$ based on the thermodynamic data reported in Yalcintas *et al.* (2016).[46] Black solid and dashed lines indicate upper and lower decomposition lines of water and "redox neutral" (pe + pH_m = 13.8) conditions. Experimental pH_m and E_h determined in the study of Kobayashi *et al.* (2013)[22] for magnetite and mackinawite systems are also included for comparison.

tigated by principal component analysis using the ITFA software package (version 1.3.12).[48] The Malinowski indicator as well as the good reconstruction of the experimental EXAFS spectra with 2 principal components (red lines in Fig. 2b and c) suggest that two structurally different Tc species are present in the magnetite samples. Based on the VARIMAX loadings, magnetite species 1 prevails in sample Mag-0, *i.e.* the structurally incorporated Tc, while magnetite species 2 prevails in sample Mag-5.

Assuming that the spectra of samples Mag-0 and -5 represent the pure endmember species, we are able to extract the noise-filtered endmember spectra of magnetite species 1 and 2 and determine their structure by shell fitting (Table 3) and to determine at the same time the relative proportions of the two species in the other samples by iterative target test (ITT) (Table 4).[48]

Subsequent shell fits are shown in Fig. S3 in the ESI.† The spectrum of magnetite species 1 could be fitted as expected by the magnetite model, with Tc(IV) residing in the 16d position of the $Fd\bar{3}m$ cubic space group. Tc is hence coordinated to 6 oxygen atoms forming the corners of a TcO_6 octahedron, which is then linked to 6 neighbouring FeO_6 octahedra by sharing edges (shorter Tc–Fe_1 distance of 3.08 Å), and to 6 next-neighbouring FeO_6 tetrahedra sharing corners (longer Tc–Fe_2 distances of 3.49 Å). A fit with floating CNs resulted in the same interatomic distances, CNs which deviated by less than 15% from the crystallographic values, hence within the typical error range, and only slightly better fit statistics (%R reduced from 6.1 to 5.3). Hence the spectrum of magnetite species 1 is fully in line with Tc(IV) residing in the 16d position of the cubic magnetite structure, *i.e.* substituting for octahedral Fe, in line with previous work.[22] Note that the Tc–O distance is 2% smaller than the Fe–O distance in magnetite (2.01 *vs.* 2.05 Å), in line with the ionic radius of Tc(IV) being smaller than that of Fe with an average oxidation state of 2.5. In contrast, the shorter Tc–Fe distance is about 4% longer than the corresponding Fe–Fe distance in magnetite (3.08 *vs.* 2.97 Å), while the longer Tc–Fe distance is almost identical (3.49 *vs.* 3.48 Å).[49] The similarity with the fit data by Um *et al.* suggests that these authors might have also observed Tc incorporation into magnetite rather than into goethite.[50]

In the FTM spectrum of magnetite species 2, most purely expressed in samples Mag-4 to -6, we observe a peak triplet from 2.0 to 3.3 Å (Fig. 2c). To elucidate the elemental identity of backscattering atoms in this region, we applied Morlet wavelet analysis.[51] The two peaks at shorter distance did not resolve in the wavelet plots, but the intensity of this unresolved wavelet peak increased up to the maximum k-range of 12.5 $Å^{-1}$, in line with backscattering atoms significantly heavier than Fe. With the known elemental composition of our system, this double peak hence can arise only from Tc–Tc backscattering. In contrast, the third peak at 3.0 Å showed a maximum at about 7.5 $Å^{-1}$, in line with backscattering by Fe.[29] Fitting this region with only two shells was, however, not sufficient: in addition to a short Tc–Tc and a long Tc–Fe_2 path, also a shorter Tc–Fe1 path was required to obtain a satisfying fit, while a second Tc–Tc path corresponding to the structure of $TcO_2{\cdot}xH_2O$ could not be fitted (Table 3). The CN of 0.8 and the distance of 2.57 Å for the Tc–Tc path suggest formation of a Tc–Tc dimer linked through the typical short, quasi-metallic bond. The two Tc–Fe distances are with 3.13 and 3.54 Å similar to the ones of structural Tc in magnetite, albeit slightly longer. Furthermore, the CN are roughly half of what would be expected for structural incorporation. The most consistent structural model based on these fit data is that of a Tc–Tc dimer, which forms on one side of the chain a tridentate sorption complex with the magnetite {111} faces, similar to that observed for trivalent Pu, As or Sb.[35,52,53] One could argue also, that the observed structure is not that of a limiting species, but represents rather a mixture of Tc-doped magnetite on one hand, and a Tc oxide species on the other hand. $TcO_2{\cdot}xH_2O(s)$ as limiting species can be excluded, however, since principal component analysis of its spectrum together with those of the magnetite samples increased the number of statistically significant components from 2 to 3. Crystalline

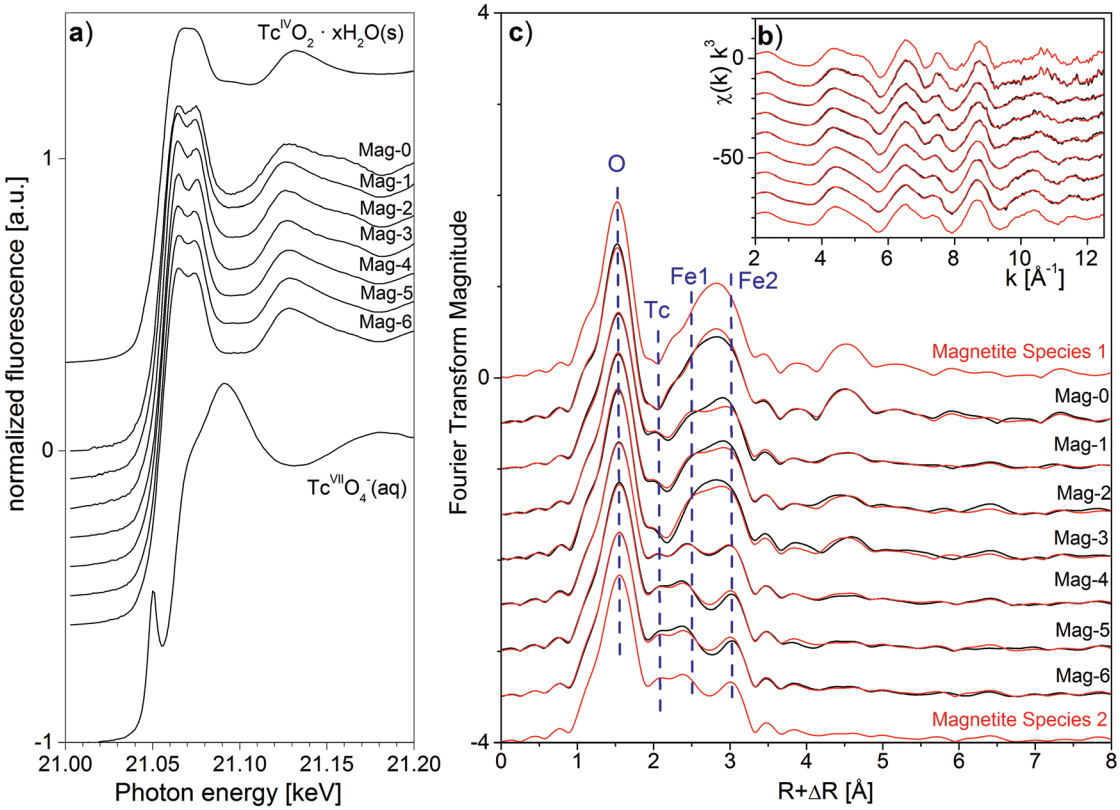

Fig. 2 Tc-K edge XAS spectra of Tc sorbed on magnetite in 0.1 M NaCl. (a) XANES, (b) k^3-weighted EXAFS spectra, (c) corresponding Fourier Transform Magnitude (FTM). Black lines represent the experimental data, the red lines in (b) and (c) represent their reconstruction with two principal components. The ITFA-derived FTM spectra of the two endmembers (magnetite species 1 and magnetite species 2) are also plotted on top and bottom, respectively.

TcO_2 can also be excluded as limiting species, since this compound has long Tc–Tc distances at 3.6–3.7 Å arising from corner-sharing linkages between the chains, which are absent in our magnetite spectra. Therefore, we maintain that the most likely structural explanation for magnetite species-2 is a Tc–Tc dimer triple-bonding to the magnetite {111} faces. This species bounds in edge-sharing bidentate mode to the ferrihydrite surface[6] and to titanomagnetite,[54] with one significant difference: while Zachara *et al.* obtained 2.57 Å for both the Tc–Tc and of the shorter Tc–Fe1 paths, and Liu *et al.* obtained 2.56 Å for Tc–Tc and 2.59 Å for Tc–Fe1, such a fitting scheme was not successful in our case, and we obtained instead much longer 3.12 Å for the shorter Tc–Fe1 path (in contrast, the distance of the longer Tc–Fe2 path is again similar, 3.50 Å (ref. 6) *vs.* 3.52 Å). This difference is not only arising from a potentially different fitting approach, but is also reflected by differences in the chi- and FTM spectra. The reason for this difference is, however, not evident.

In our magnetite series, the contribution of structural Tc(IV) increases from 1/3 to 1/2 for samples Mag-1 to -3, *i.e.* increases with Tc loading for the samples prepared with the lower initial TcO_4^- concentration of 2×10^{-5} M, while the contribution of the sorption complex decreases correspondingly. In the samples Mag-4 to -6 with the higher TcO_4^- concentrations, the sorption complex prevails. Our hypothesis is that the amount of Tc–Tc dimers increases at the given pH of ~9 with initial Tc concentration, thereby competing with the sorption of monomers or their structural incorporation. In principle, these dimers may form either in solution or at the magnetite surface. However, reduction of Tc(VII) to Tc(IV) by Fe(II) in solution is unlikely and known as kinetically hindered process.[17] Therefore, dimer formation should proceed prevalently at the (semiconducting to conducting) magnetite surface. This, however, seems to be in contradiction to the increase of structural Tc with increasing Tc surface loading as observed for samples Mag-1 to -3.

As discussed in the introduction, both complete incorporation of Tc into the magnetite structure and formation of TcO_2-like dimers/polymers on the surface were reported by different authors.[6,7,21,22,55] However, none of the available studies has systematically investigated the effect of initial Tc concentration and solid to liquid ratio (or loading) as accomplished in the present work, but rather focussed on a given [Tc] and loading. Kobayashi and co-workers[22] conducted Tc uptake experiments with magnetite under analogous $[Tc]_0$ and loading (2×10^{-5} M and 400 ppm, respectively), but significantly lower pH values (6–7.5). The authors observed the complete incorporation of Tc(IV) in the structure of magnetite. The differences in the prevailing uptake mechanism observed in this work and in Kobayashi *et al.* are interpreted in connection

Table 3 EXAFS-derived structural parameters for Tc in the magnetite and mackinawite series

Sample	Path	CN[a]	R (Å)	σ^2 (Å^2)	ΔE° (eV)	%R^b
Magnetite Species 1 (Structural Tc(IV))	Tc–O	6[f]	2.01	0.0043	3.0	6.1
	Tc–Fe_1	6[f]	3.08	0.0113		
	Tc–Fe_2	6[f]	3.49	0.0093		
Magnetite Species 2 (Sorbed Tc(IV) dimers)	Tc–O	5.7	2.02	0.0037	3.9	6.7
	Tc–Tc	0.9	2.57	0.0018		
	Tc–Fe_1	2.9	3.12	0.0100[c]		
	Tc–Fe_2	4.4	3.52	0.0100[c]		
Mackinawite Species 1 (TcS_x)	Tc–S	5.8	2.38	0.0092	8.2	9.7
	Tc–Tc	0.8	2.83	0.0032		
Mackinawite Species 2 ($TcO_2{\cdot}xH_2O$(s)) Model 1	Tc–O_1	4[f]	2.00	0.0025	−0.9	9.3
	Tc–O_2	2[f]	2.38	0.0010		
	Tc–Tc	2[f]	2.55	0.0032		
	MS	4[f]	4.03	0.0071		
Mackinawite Species 2 ($TcO_2{\cdot}xH_2O$(s)) Model 2	Tc–O_1	4[f]	2.00	0.0024	−0.7	8.4
	Tc–O_2	2[f]	2.38	0.0015		
	Tc–Tc_1	1[f]	2.54	0.0040		
	Tc–Tc_2	1[f]	3.01	0.0099		
	MS	4[f]	4.01	0.0051		
TcO_4^- (aq)[47]	Tc–O	4	1.72	0.0014	9.5	9.2

[a] CN (coordination number). [b] R (residual). Fit errors: CN: ±25%; R: 0.01 Å, σ^2: 0.002 Å^2, f: fixed, c: constrained.

Table 4 Quantitative speciation of the Tc magnetite samples based on EXAFS-ITFA. Bold numbers indicate fixed values

Sample	Fraction magnetite species 1: structural Tc(IV)	Fraction magnetite species 2: sorbed Tc(IV) dimers	Sum
Mag-0	**1.00**	**0.00**	**1.00**
Mag-1	0.33	0.59	0.92
Mag-2	0.42	0.53	0.95
Mag-3	0.54	0.47	1.01
Mag-4	0.15	0.82	0.97
Mag-5	**0.00**	**1.00**	**1.00**
Mag-6	0.02	0.97	0.99

with differences in magnetite solubility in both systems. As shown in Fig. 3, the solubility of magnetite in the pH_m range 6–7.5 (pe + pH_m = 4, see Fig. 1) (Kobayashi *et al.*, 2013) is significantly larger than at pH_m ~9 (pe + pH_m = 7, see Fig. 1) (this work). Higher concentrations of Fe in solution are expected to promote a greater recrystallization rate, thus facilitating the incorporation of Tc(IV) in the structure of magnetite. These observations strongly suggest that the mechanism driving the retention of Tc by magnetite strongly depends on the initial Tc concentration and pH, and to a lesser extent on the loading on the surface of magnetite.

Mackinawite. Fig. 4a shows the Tc K-edge XANES spectra of Mack-1 to Mack-6, corresponding to Tc sorbed on mackinawite. As in the case of Tc uptake by magnetite, all investigated mackinawite samples do not show the pre-edge feature at 21.05 keV characteristic of Tc(VII), thus indicating the complete (>95%) reduction of Tc(VII) to Tc(IV) within the timeframe of the experiment. The XANES spectral features are, however,

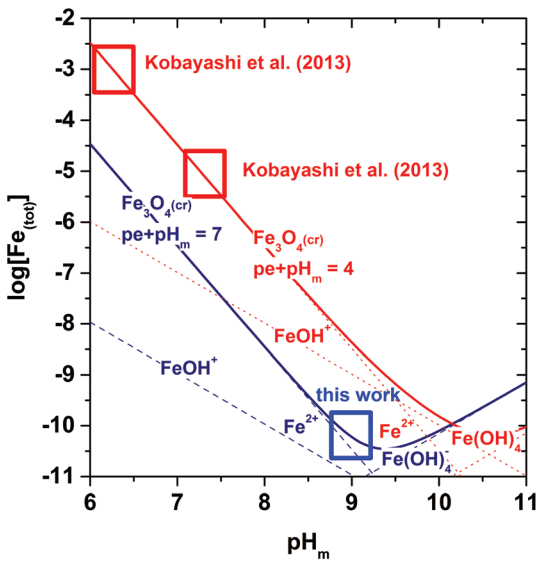

Fig. 3 Solubility of magnetite (Fe_3O_4(cr)) calculated for pe + pH_m = 4 (red, Kobayashi *et al.*, 2013) and pe + pH_m = 7 (blue, this work) using ThermoChimie TDB.[56]

different from those of the magnetite samples in several aspects, most notably the absence of the splitting of the white line peak. The spectral differences between the magnetite and the mackinawite samples are even more pronounced when looking at the EXAFS spectra (Fig. 4b and c). As before, the series of EXAFS spectra was analysed by ITFA to derive the number of spectral components present. The Malinowski indicator values and the reconstruction of the experimental spectra suggested the presence of two spectral components

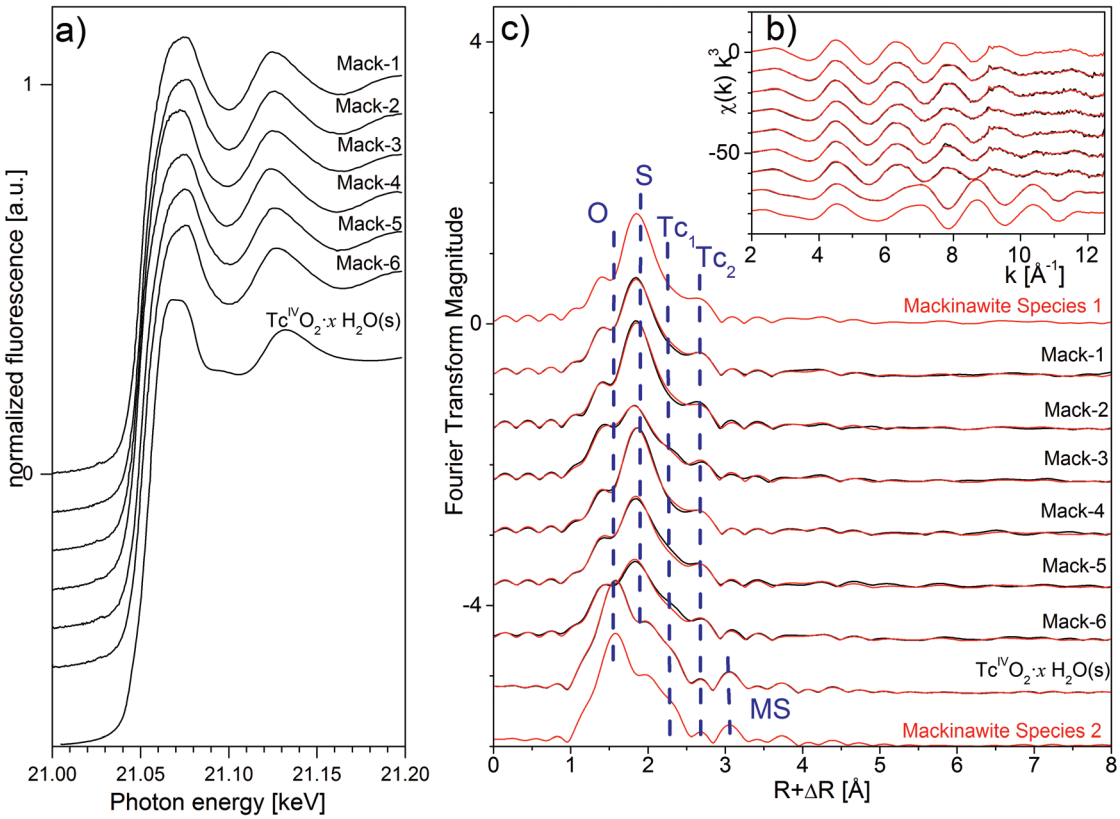

Fig. 4 Tc-K edge XAS spectra of Tc sorbed on mackinawite in 0.1 M NaCl (a) XANES, (b) k^3-weighted EXAFS spectra, and (c) corresponding Fourier Transform magnitude. Black lines represent the experimental data, the red lines in (b) and (c) represent their reconstruction with two principal components.

and hence Tc species (Fig. 4b and c). Also in contrast to the magnetite samples, the addition of the $TcO_2{\cdot}xH_2O$(s) reference did not increase the number of factors, demonstrating that $TcO_2{\cdot}xH_2O$(s) is one of the two components present, albeit as a relatively small fraction, since none of the mackinawite (XANES and EXAFS) spectra is a close match of the $TcO_2{\cdot}xH_2O$(s) reference.

The spectral component of the non-TcO_2-species is most purely expressed in sample Mack-4 based on the VARIMAX factor loading. This EXAFS spectrum – as well as that of the other mackinawite samples – is dominated by a FTM peak at about 1.9 Å (labelled "S"), *i.e.* about 0.3 Å more than that of the Tc(IV)–O coordination peak (labelled "O"), suggesting sulphur instead of oxygen coordination. The EXAFS shell fit of the ITFA-derived endmember spectrum (Mackinawite species 1, see also Fig. S4†) using FEFF 8.2 calculated paths of an atomic cluster based on the structure of TcS_2 [57] confirmed sulphur in sixfold coordination to Tc at a distance of 2.38 Å, which is very close to the average distance of the TcS_2 coordination shell at 2.393 Å (Table 4). A second FTM peak at about 2.6 Å (labelled "Tc_2") could be fitted with one Tc atom at 2.83 Å, *i.e.* only one of the expected three Tc neighbours in the distal range 2.79–2.90 Å of TcS_2 could be fitted. Indeed, the local structure of the species formed in presence of mackinawite is more similar to Tc_2S_7 or TcS_x previously observed in comparable systems.[58,59] This is corroborated by the Tc–S distance of 2.38 Å in line with that of Lukens *et al.* and an only slightly longer Tc–Tc distance of 2.83 Å, which has been reported as 2.77 Å by Lukens *et al.* Our coordination numbers are also slightly smaller (6 instead of 7, and 1 instead of 2 for Tc–S and Tc–Tc, respectively). Whether these small discrepancies arise from shell fit uncertainties or from small structural differences is not easy to decide, but there is no doubt that mackinawite species 1 is largely in line with the previously observed TcS_x, and not with the high-temperature phase TcS_2.[60]

Mackinawite species 2, which corresponds to $TcO_2{\cdot}xH_2O$(s) demonstrated by ITFA as described before, was fitted following the model first suggested by Lukens *et al.*[61] In this one-dimensional chain structure, strongly distorted $TcO_4(OH_2)_6$ octahedra are linked by uniform Tc–Tc bonds of about 2.57 Å and two Tc–O bonds of about 2.02 Å in a square planar arrangement. Two longer Tc–O paths of about 2.47 Å arise from bonding water molecules above and below the TcO_4 squares, which complete the octahedral coordination of Tc^{IV}. The fit requires also a four-legged multiple scattering path (MS) arising from the square planar arrangement of the TcO_4 units. The resulting bond lengths and corresponding Debye–Waller factors, reported in Table 3 as model 1, are largely in line with previously published results.[21,61,62] In an alternative attempt, we adopted again the square planar configuration including the split of the TcO_6 coordination shell in two Tc–O distances

Table 5 Quantitative speciation of the Tc mackinawite samples based on EXAFS-ITFA. Bold numbers indicate fixed values

Sample	Fraction mackinawite species 1: $Tc^{IV}S_x$	Fraction mackinawite species 2: $TcO_2{\cdot}xH_2O$(s)	Sum
Mack-1	0.93	0.07	1.00
Mack-2	0.99	0.01	1.00
Mack-3	0.79	0.21	1.00
Mack-4	**1.00**	**0.00**	**1.00**
Mack-5	0.89	0.11	1.00
Mack-6	0.82	0.18	1.00
$TcO_2{\cdot}xH_2O$(s)	**0.00**	**1.00**	**1.00**

and the arising MS path, but allowed for the alternating longer and shorter Tc–Tc distances along the chains like in crystalline TcO_2.[59] While the Tc–O distances remain identical to those of model 1, the Tc–Tc distances show a clear splitting, a shorter at 2.54 Å and a longer at 3.01 Å (model 2 in Table 3). The shorter distance is within the error limit identical to that of model 1, and both distances are 2–3% smaller than those of crystalline TcO_2 (2.62 and 3.08 Å). Both models provide a good fit in terms of fit statistics and physically meaningful data; the second model is slightly better, however, based on the smaller error and the length of the MS path being closer to the value of 4.00 Å expected from the fitted average Tc–O distance of 2.00 Å. From a crystal-chemical point of view, the short-long Tc pairing scheme is based on a sensitive balance between crystal field stabilization (favoring an even distribution of Tc–Tc distances by stabilizing a more symmetric TcO_6 octahedron, t_{2g}^3 configuration) and valence electrons available to form a Tc–Tc metal bond (shortening one of the two Tc–Tc distances).[63,64]

In contrast to the EXAFS-ITFA-derived Tc speciation in the magnetite system, which showed an effect of the initial Tc concentration, the Tc speciation of the mackinawite series established in the same way shows rather an effect of Tc surface loading: samples Mack-3 and Mack-6 with the highest loading of 900 ppm have the highest contribution of $TcO_2{\cdot}xH_2O$(s), although it never exceeds 20%, while the TcS_x-like phase prevails in all systems (Table 5).

Analogous species/moieties were previously reported in the literature, based on spectroscopic evidences obtained under different experimental conditions. Kobayashi *et al.*[22] suggested the formation of a TcS_2-like phase based on their XANES data, in experiments conducted with $[Tc]_0 = 2 \times 10^{-5}$ M and 200 ppm Tc loading. With a significantly higher loading (99 000 ppm) and $[Tc]_0$ (1.5×10^{-4} M), Liu *et al.*[28] reported the immobilization of Tc by mackinawite as a TcO_2-like phase (Tc–O path at 1.99 ± 0.02 Å with CN = 6). Provided the very high loading and $[Tc]_0$, the main component is identified as $TcO_2{\cdot}xH_2O$(s) by Liu and co-workers. These observations are in line with our experimental data and spectroscopic findings: (i) there is a clear and systematic effect of loading on the retention of Tc by mackinawite; (ii) a component with predominance of Tc–S interactions in the first shell forms in mackinawite systems with low Tc loadings; (iii) a $TcO_2{\cdot}xH_2O$(s) phase (either surface precipitate or colloid) starts to form with increasing loading, becoming predominant at the very high loadings used by Liu and co-workers (99 000 ppm). Note that the method of mackinawite synthesis used in our work is identical to that of Kobayashi *et al.* (2013)[22] and Liu *et al.* (2008).[28]

In contrast to these observations, Livens *et al.*[27] reported the formation of a TcS_2-like phase (d_{Tc-S} = 2.42 ± 0.02 Å and CN = 6) in the presence of relatively high loadings (10 000 ppm) of Tc on 300 mg mackinawite. A direct comparison of the data by Livens and co-workers with the present study cannot be accomplished, provided the different method used for the synthesis of mackinawite and the very limited experimental description provided by the authors, which omits (among others) information on S : L, $[Tc]_0$ and pH.

Conclusions

Tc reduction and uptake mechanisms by Fe(II) minerals (magnetite and mackinawite) were investigated in 0.1 M NaCl systems. The results show that Tc(VII) is reduced to Tc(IV) in contact with magnetite and mackinawite in all investigated systems regardless of initial $[Tc]_0$ and solid-to-liquid ratio. The observed reduction is also consistent with the thermodynamically calculated Tc(VII)/Tc(IV) borderline.

EXAFS data evaluation indicates that the mechanisms of Tc(IV) retention by magnetite and mackinawite are strongly dependent on the loading, $[Tc]_0$ and pH_m. Tc(IV) partly incorporates into the structure of magnetite at low $[Tc]_0$ (2×10^{-5} M), but forms Tc-Tc dimers bonding to the magnetite {111} face at $[Tc]_0 = 2 \times 10^{-4}$ M. A full incorporation of Tc into the magnetite structure is triggered by boundary conditions enhancing magnetite solubility (and thus promoting a greater recrystallization degree), *e.g.* lower pH_m and E_h values. In contrast to magnetite, $[Tc]_0$ has no clear impact on the uptake of Tc by mackinawite. A TcS_x-like phase prevails in all investigated mackinawite systems, although the contribution of up to ~20% of $TcO_2{\cdot}xH_2O$(s) (likely as surface precipitate) is observed for the highest investigated loadings (900 ppm).

These results provide key inputs for the understanding of the mechanisms driving the reduction and retention of Tc by magnetite and mackinawite under repository-relevant conditions, whilst highlighting the need of coupling classical wet-chemistry techniques, thermodynamic calculations and advanced spectroscopic methods when investigating complex processes or systems such as redox and mineral interfaces.

Acknowledgements

The technical support of M. Böttle (KIT-INE) is kindly acknowledged. The assistance of André Rossberg (ESRF-ROBL) and Christoph Hennig (ESRF-ROBL) during EXAFS measurements is highly appreciated. We would like to acknowledge Prof. Dr Shijun Wu for the preparation of $TcO_2{\cdot}xH_2O$ solid phase used as a reference material in (ESRF-ROBL). Prof. Dr Horst Geckeis is thankfully acknowledged for the fruitful scientific discussions and the support in the development of this study.

This work was funded by the German Federal Ministry of Economics and Technology (BMWi) under the project of VESPA.

References

1 C. D. Russell and A. Cash, Products of pertechnetate reduction in complexing media, *J. Nucl. Med.*, 1978, **19**(6), 694–694.
2 J. Grassi, P. Rogelet, J. Devynck and B. Tremillon, Radiopolarography of technetium(VII) in acidic medium, *J. Electroanal. Chem.*, 1978, **88**(1), 97–103.
3 J. Grassi, J. Devynck and B. Tremillon, Electrochemical studies of technetium at a mercury-electrode, *Anal. Chim. Acta*, 1979, **107**(Jun), 47–58.
4 F. Poineau, M. Fattahi, C. Den Auwer, C. Hennig and B. Grambow, Speciation of technetium and rhenium complexes by in situ XAS-electrochemistry, *Radiochim. Acta*, 2006, **94**(5), 283–289.
5 *Chemical thermodynamics of technetium*, ed. J. A. Rard, M. H. Rand, G. Anderegg and H. Wanner, Elsevier, North-Holland, Amsterdam, 1999.
6 J. M. Zachara, S. M. Heald, B. H. Jeon, R. K. Kukkadapu, C. X. Liu, J. P. McKinley, A. C. Dohnalkova and D. A. Moore, Reduction of pertechnetate [Tc(VII)] by aqueous Fe(II) and the nature of solid phase redox products, *Geochim. Cosmochim. Acta*, 2007, **71**(9), 2137–2157.
7 T. S. Peretyazhko, J. M. Zachara, R. K. Kukkadapu, S. M. Heald, I. V. Kutnyakov, C. T. Resch, B. W. Arey, C. M. Wang, L. Kovarik, J. L. Phillips and D. A. Moore, Pertechnetate (TcO_4^-) reduction by reactive ferrous iron forms in naturally anoxic, redox transition zone sediments from the Hanford Site, USA, *Geochim. Cosmochim. Acta*, 2012, **92**, 48–66.
8 J. H. Lee, J. M. Zachara, J. K. Fredrickson, S. M. Heald, J. P. McKinley, A. E. Plymale, C. T. Resch and D. A. Moore, Fe(II)- and sulfide-facilitated reduction of $^{99}Tc(VII)O_4^-$ in microbially reduced hyporheic zone sediments, *Geochim. Cosmochim. Acta*, 2014, **136**, 247–264.
9 R. E. Wildung, S. W. Li, C. J. Murray, K. M. Krupka, Y. Xie, N. J. Hess and E. E. Roden, Technetium reduction in sediments of a shallow aquifer exhibiting dissimilatory iron reduction potential, *FEMS Microbiol. Ecol.*, 2004, **49**(1), 151–162.
10 I. T. Burke, C. Boothman, J. R. Lloyd, F. R. Livens, J. M. Charnock, J. M. McBeth, R. J. G. Mortimer and K. Morris, Reoxidation behavior of technetium, iron, and sulfur in estuarine sediments, *Environ. Sci. Technol.*, 2006, **40**(11), 3529–3535.
11 I. T. Burke, C. Boothman, J. R. Lloyd, R. J. G. Mortimer, F. R. Livens and K. Morris, Effects of progressive anoxia on the solubility of technetium in sediments, *Environ. Sci. Technol.*, 2005, **39**(11), 4109–4116.
12 I. T. Burke, F. R. Livens, J. R. Lloyd, A. P. Brown, G. T. W. Law, J. M. McBeth, B. L. Ellis, R. S. Lawson and K. Morris, The fate of technetium in reduced estuarine sediments: Combining direct and indirect analyses, *Appl. Geochem.*, 2010, **25**(2), 233–241.
13 J. M. McBeth, G. Lear, J. R. Lloyd, F. R. Livens, K. Morris and I. T. Burke, Technetium reduction and reoxidation in aquifer sediments, *Geomicrobiol. J.*, 2007, **24**(3–4), 189–197.
14 V. Metz, H. Geckeis, E. Gonzalez-Robles, A. Loida, C. Bube and B. Kienzler, Radionuclide behaviour in the near-field of a geological repository for spent nuclear fuel, *Radiochim. Acta*, 2012, **100**(8–9), 699–713.
15 *Aquatic chemistry of long-lived mobile fission and activation products in the context of deep geological disposal*, ed. A. Abdelouas and B. Grambow, Woodhead Publishing, Cambridge, UK, 2012.
16 D. Q. Cui and T. E. Eriksen, Reduction of pertechnetate in solution by heterogeneous electron transfer from Fe(II)-containing geological material, *Environ. Sci. Technol.*, 1996, **30**(7), 2263–2269.
17 D. Q. Cui and T. E. Eriksen, Reduction of pertechnetate by ferrous iron in solution: Influence of sorbed and precipitated Fe(II), *Environ. Sci. Technol.*, 1996, **30**(7), 2259–2262.
18 K. Morris, F. R. Livens, J. M. Charnock, I. T. Burke, J. M. McBeth, J. D. C. Begg, C. Boothman and J. R. Lloyd, An X-ray absorption study of the fate of technetium in reduced and reoxidised sediments and mineral phases, *Appl. Geochem.*, 2008, **23**(4), 603–617.
19 K. Geraedts, C. Bruggeman, A. Maes, L. R. Van Loon, A. Rossberg and T. Reich, Evidence for the existence of Tc(IV) - humic substance species by X-ray absorption near-edge spectroscopy, *Radiochim. Acta*, 2002, **90**(12), 879–884.
20 K. Geraedts and A. Mais, Determination of the conditional interaction constant between colloidal technetium(IV) and Gorleben humic substances, *Appl. Geochem.*, 2008, **23**(5), 1127–1139.
21 A. Maes, K. Geraedts, C. Bruggeman, J. Vancluysen, A. Rossberg and C. Hennig, Evidence for the interaction of technetium colloids with humic substances by X-ray absorption spectroscopy, *Environ. Sci. Technol.*, 2004, **38**(7), 2044–2051.
22 T. Kobayashi, A. C. Scheinost, D. Fellhauer, X. Gaona and M. Altmaier, Redox behavior of Tc(VII)/Tc(IV) under various reducing conditions in 0.1 M NaCl solutions, *Radiochim. Acta*, 2013, **101**(5), 323–332.
23 T. A. Marshall, K. Morris, G. T. W. Law, J. F. W. Mosselmans, P. Bots, S. A. Parry and S. Shaw, Incorporation and Retention of 99-Tc(IV) in Magnetite under High pH Conditions, *Environ. Sci. Technol.*, 2014, **48**(20), 11853–11862.
24 E. Yalcintas, X. Gaona, A. C. Scheinost, T. Kobayashi, M. Altmaier and H. Geckeis, Redox chemistry of Tc(VII)/Tc(IV) in dilute to concentrated NaCl and $MgCl_2$ solutions, *Radiochim. Acta*, 2015, **103**(1), 57–72.
25 F. N. Smith, W. Um, C. D. Taylor, D. Kim, M. J. Schweiger and A. A. Kruger, Computational investigation of technetium (IV) incorporation into inverse spinels: magnetite

(Fe_3O_4) and trevorite ($NiFe_2O_4$), *Environ. Sci. Technol.*, 2016, **50**(10), 5216–5224.

26 M. J. Wharton, B. Atkins, J. M. Charnock, F. R. Livens, R. A. D. Pattrick and D. Collison, An X-ray absorption spectroscopy study of the coprecipitation of Tc and Re with mackinawite (FeS), *Appl. Geochem.*, 2000, **15**(3), 347–354.

27 F. R. Livens, M. J. Jones, A. J. Hynes, J. M. Charnock, J. F. W. Mosselmans, C. Hennig, H. Steele, D. Collison, D. J. Vaughan, R. A. D. Pattrick, W. A. Reed and L. N. Moyes, X-ray absorption spectroscopy studies of reactions of technetium, uranium and neptunium with mackinawite, *J. Environ. Radioact.*, 2004, **74**(1–3), 211–219.

28 Y. Liu, J. Terry and S. Jurisson, Pertechnetate immobilization with amorphous iron sulfide, *Radiochim. Acta*, 2008, **96**(12), 823–833.

29 A. C. Scheinost, R. Kirsch, D. Banerjee, A. Fernandez-Martinez, H. Zaenker, H. Funke and L. Charlet, X-ray absorption and photoelectron spectroscopy investigation of selenite reduction by Fe-II-bearing minerals, *J. Contam. Hydrol.*, 2008, **102**(3–4), 228–245.

30 R. Kirsch, D. Fellhauer, M. Altmaier, V. Neck, A. Rossberg, L. Charlet and A. C. Scheinost, Reaction of Pu(III) and (V) with magnetite and mackinawite: A XANES/EXAFS investigation, *Geochim. Cosmochim. Acta*, 2010, **74**(12), A520–A520.

31 S. Dulnee, D. Banerjee, B. J. Merkel and A. C. Scheinost, Surface Complexation and Oxidation of Sn-II by Nanomagnetite, *Environ. Sci. Technol.*, 2013, **47**(22), 12852–12859.

32 S. Dulnee and A. C. Scheinost, Interfacial reaction of Sn-II on mackinawite (FeS), *J. Contam. Hydrol.*, 2015, **177**, 183–193.

33 H. E. Swanson, H. F. McMurdie, M. C. Morris and E. H. Evans, *Standart X-ray diffraction powder patterns*, U.S. Department of Commerce, 1967.

34 T. E. Howard, C. Milton, E. C. T. Chao, I. Adler, C. Mead, B. Ingram and R. Berner, Valleriite and the new iron sulfide, mackinawite, *Mineral. Petrol.*, 1964, **475-D**, D64–D69.

35 R. Kirsch, D. Fellhauer, M. Altmaier, V. Neck, A. Rossberg, T. Fanghänel, L. Charlet and A. C. Scheinost, Oxidation state and local structure of plutonium reacted with magnetite, mackinawite and chukanovite, *Environ. Sci. Technol.*, 2011, **45**(17), 7267–7274.

36 *Iron Oxides in the Laboratory*, ed. U. Schwertmann and R. M. Cornell, Weinheim, Germany, 2000.

37 M. Altmaier, V. Metz, V. Neck, R. Muller and T. Fanghänel, Solid-liquid equilibria of $Mg(OH)_2$(cr) and $Mg_2(OH)_3Cl.4H_2O$(cr) in the system Mg-Na-H-OH-O-Cl-H_2O at 25 °C, *Geochim. Cosmochim. Acta*, 2003, **67**(19), 3595–3601.

38 C. M. Nelson, G. E. Boyd and W. T. Smith, Magnetochemistry of Technetium and Rhenium, *J. Am. Chem. Soc.*, 1954, **76**(2), 348–352.

39 X. Gaona, R. Dahn, J. Tits, A. C. Scheinost and E. Wieland, Uptake of Np(IV) by C-S-H phases and cement paste: an EXAFS study, *Environ. Sci. Technol.*, 2011, **45**(20), 8765–8771.

40 S. M. Webb, SIXpack: a graphical user interface for XAS analysis using IFEFFIT, *Phys. Scr.*, 2005, **T115**, 1011–1014.

41 T. Ressler, WinXAS: a program for X-ray absorption spectroscopy data analysis under MS-Windows, *J. Synchrotron Radiat.*, 1998, **5**, 118–122.

42 A. Rossberg, T. Reich and G. Bernhard, Complexation of uranium(VI) with protocatechuic acid - application of iterative transformation factor analysis to EXAFS spectroscopy, *Anal. Bioanal. Chem.*, 2003, **376**(5), 631–638.

43 A. Rossberg, K. U. Ulrich, S. Weiss, S. Tsushima, T. Hiemstra and A. C. Scheinost, Identification of Uranyl Surface Complexes an Ferrihydrite: Advanced EXAFS Data Analysis and CD-MUSIC Modeling, *Environ. Sci. Technol.*, 2009, **43**(5), 1400–1406.

44 A. C. Scheinost, A. Rossberg, D. Vantelon, I. Xifra, R. Kretzschmar, A. K. Leuz, H. Funke and C. A. Johnson, Quantitative antimony speciation in shooting-range soils by EXAFS spectroscopy, *Geochim. Cosmochim. Acta*, 2006, **70**(13), 3299–3312.

45 B. Ravel and M. Newville, ATHENA, ARTEMIS, HEPHAESTUS: data analysis for X-ray absorption spectroscopy using IFEFFIT, *J. Synchrotron Radiat.*, 2005, **12**, 537–541.

46 E. Yalcintas, X. Gaona, M. Altmaier, K. Dardenne, R. Polly and H. Geckeis, Thermodynamic description of Tc(IV) solubility and hydrolysis in dilute to concentrated NaCl, $MgCl_2$ and $CaCl_2$ solutions, *Dalton Trans.*, 2016, **45**, 8916–8936.

47 M. Saeki, Y. Sasaki, A. Nakai, A. Ohashi, D. Banerjee, A. C. Scheinost and H. Foerstendorf, Structural study on complex of MIDOA with $M(VII)O_4^-$ (M=Re and Tc) by ^{1}H-NMR, EXAFS and IR spectroscopy, *Inorg. Chem.*, 2012, **51**(10), 5814–5821.

48 A. C. Scheinost, C. Hennig, A. Somogyi, G. Martinez-Criado and R. Knappik, Geochemical behavior of uranium in mine tailings at Freital, Germany: A mu-XRF, mu-XAFS and mu-XRD study, *Geochim. Cosmochim. Acta*, 2006, **70**(18), A560–A560.

49 M. E. Fleet, The Structure of Magnetite - Symmetry of Cubic Spinels, *J. Solid State Chem.*, 1986, **62**(1), 75–82.

50 W. Um, H. S. Chang, J. P. Icenhower, W. W. Lukens, R. J. Serne, N. P. Qafoku, J. H. Westsik, E. C. Buck and S. C. Smith, Immobilization of 99-Technetium (VII) by Fe(II)-Goethite and Limited Reoxidation, *Environ. Sci. Technol.*, 2011, **45**(11), 4904–4913.

51 H. Funke, A. C. Scheinost and M. Chukalina, Wavelet analysis of extended X-ray absorption fine structure data, *Phys. Rev. B: Condens. Matter*, 2005, **71**, 094110.

52 R. Kirsch, A. C. Scheinost, A. Rossberg, D. Banerjee and L. Charlet, Reduction of antimony by nano-particulate magnetite and mackinawite, *Mineral. Mag.*, 2008, **72**(1), 185–189.

53 Y. H. Wang, G. Morin, G. Ona-Nguema, N. Menguy, F. Juillot, E. Aubry, F. Guyot, G. Calas and G. E. Brown, Arsenite sorption at the magnetite-water interface during aqueous precipitation of magnetite: EXAFS evidence for a

new arsenite surface complex, *Geochim. Cosmochim. Acta*, 2008, **72**(11), 2573–2586.

54 J. Liu, C. I. Pearce, O. Qafoku, E. Arenholz, S. M. Heald and K. M. Rosso, Tc(VII) reduction kinetics by titanomagnetite ($Fe_{3-x}Ti_xO_4$) nanoparticles, *Geochim. Cosmochim. Acta*, 2012, **92**, 67–81.

55 J. M. McBeth, J. R. Lloyd, G. T. W. Law, F. R. Livens, I. T. Burke and K. Morris, Redox interactions of technetium with iron-bearing minerals, *Mineral. Mag.*, 2011, **75**(4), 2419–2430.

56 E. Giffaut, M. Grive, P. Blanc, P. Vieillard, E. Colas, H. Gailhanou, S. Gaboreau, N. Marty, B. Made and L. Duro, Andra thermodynamic database for performance assessment: ThermoChimie, *Appl. Geochem.*, 2014, **49**, 225–236.

57 H. J. Lamfers, A. Meetsma, G. A. Wiegers and J. L. deBoer, The crystal structure of some rhenium and technetium dichalcogenides, *J. Alloys Compd.*, 1996, **241**(1–2), 34–39.

58 W. W. Lukens, J. J. Bucher, D. K. Shuh and N. M. Edelstein, Evolution of technetium speciation in reducing grout, *Environ. Sci. Technol.*, 2005, **39**(20), 8064–8070.

59 Y. Liu, J. Terry and S. Jurisson, Pertechnetate immobilization in aqueous media with hydrogen sulfide under anaerobic and aerobic environments, *Radiochim. Acta*, 2007, **95**(12), 717–725.

60 J. C. Wildervanck and F. Jellinek, Dichalcogenides of Technetium and Rhenium, *J. Less-Common Met.*, 1971, **24**(1), 73–81.

61 W. W. Lukens, J. J. Bucher, N. M. Edelstein and D. K. Shuh, Products of pertechnetate radiolysis in highly alkaline solution: Structure of $TcO_2.H_2O$, *Environ. Sci. Technol.*, 2002, **36**(5), 1124–1129.

62 L. Vichot, G. Ouvrard, G. Montavon, M. Fattahi, C. Musikas and B. Grambow, XAS study of technetium(IV) polymer formation in mixed sulphate/chloride media, *Radiochim. Acta*, 2002, **90**(9–11), 575–579.

63 E. E. Rodriguez, F. Poineau, A. Llobet, A. P. Sattelberger, J. Bhattacharjee, U. V. Waghmare, T. Hartmann and A. K. Cheetham, Structural studies of TcO_2 by neutron powder diffraction and first-principles calculations, *J. Am. Chem. Soc.*, 2007, **129**(33), 10244–10248.

64 J. K. Burdett, Electronic Control of the Geometry of Rutile and Related Structures, *Inorg. Chem.*, 1985, **24**(14), 2244–2253.